PERGAMON

Vision Research 38 (1998) 1967–1982

Vision Research

Vernier and letter acuities for low-pass filtered moving stimuli

Susana T.L. Chung *, Harold E. Bedell

College of Optometry, University of Houston, Houston, TX 77204, USA

Received 7 February 1997; received in revised form 8 September 1997

Abstract

Vernier and letter acuities are both susceptible to degradation by image motion. In a previous study, we showed that the worsening of Vernier acuity for stimuli moving up to 4°/s is accounted for primarily by a shift of visual sensitivity to mechanisms of lower spatial frequency. The purposes of this study were to extend the previous results for Vernier acuity to higher stimulus contrast and velocities, and to determine if a shift in spatial scale can similarly explain the degradation of letter acuity for moving stimuli. We measured *Vernier discrimination* for a pair of vertical abutting thin lines and *letter resolution* for a four-orientation letter 'T' as a function of stimulus velocity ranging from 0 to 12°/s. Stimuli were presented at 20 times the detection threshold, determined for each velocity. To determine the spatial-frequency mechanism that mediates each task at each velocity, we measured Vernier and letter acuities with low-pass filtered stimuli (cut-off spatial-frequency: 17.1–1.67 c/deg) and analyzed the data using an equivalent blur analysis. Our results show that the empirically determined, equivalent intrinsic blur associated with both tasks increases as a function of stimulus velocity, suggesting corresponding increases in the size of optimally responding mechanisms. This progressive increase in mechanism size can account for the worsening of Vernier and letter acuities with velocity. Vernier discrimination is found to be more susceptible to degradation by various stimulus parameters than letter resolution, suggesting that different mechanisms are involved in the two tasks. We conclude that the elevations in Vernier and letter acuities for moving stimuli are the consequence of a shift of visual sensitivity toward mechanisms of lower spatial frequencies.

Keywords: Vernier acuity; Letter acuity; Motion; Low-pass filtering; Intrinsic blur

1. Introduction

Our ability to see the fine details of objects diminishes when the target of interest moves at a high speed (e.g. [1]). Under optimal conditions of high stimulus contrast and luminance, spatial thresholds such as Vernier and resolution acuities are degraded only by image motion faster than 2–3°/s (e.g. [1–5]). For low-contrast targets, Vernier thresholds are degraded at even lower velocities [6]. However, despite the well-documented degradation of spatial thresholds by image motion, the effect is not well understood in terms of our knowledge of spatial and temporal vision.

In an earlier study, we used a masking paradigm to identify the band of spatial frequencies that is most crucial for mediating Vernier discrimination at various velocities [6]. The masking data implicated a shift in the spatial scale of analysis as the principal factor in accounting for the elevated Vernier thresholds for moving stimuli. The basis for a shift in the spatial scale of analysis derives from the spatio-temporal properties of the human visual system (e.g. [7–11]). Specifically, low spatial-frequency mechanisms are more sensitive to moving stimuli than their high spatial-frequency counterparts. Thus, spatial thresholds measured for moving stimuli would be expected to be mediated primarily by low spatial-frequency mechanisms, which operate at larger spatial scales. Recent studies by Levi and his co-workers provide evidence to show that elevated Vernier thresholds in amblyopes and the normal periphery can be explained by a shift of the spatial scale toward lower spatial frequencies [12,13]. As argued by Levi and his co-workers [12,13], a shift in spatial scale toward lower spatial frequencies causes an elevation in Vernier thresholds because the precision of spatial localization depends on the slope (the change in sensitiv-

* Corresponding author. Present address: School of Optometry, Indiana University, Bloomington, IN 47405, USA. E-mail: chung@indiana.edu.

0042-6989/98/$19.00
PII: S0042-6989(97)00327-1

ity with position) of the spatial tuning function of the responding mechanism [14–16].

Recently, Morgan and Castet [17] proposed that thresholds for moving targets are subject to a temporal-frequency limitation. They measured stereoscopic thresholds using low-spatial frequency sine-wave gratings and found that these thresholds remain constant until the temporal frequency of motion exceeds a limit of 30–40 Hz. The importance of temporal frequency as a factor that limits spatial thresholds for moving targets is supported by two other recent studies. Levi [18] demonstrated that Vernier thresholds for low-spatial frequency, sine-wave gratings are approximately constant until the motion exceeds a temporal frequency of 10 Hz. Previously, we showed that Vernier thresholds for mid-spatial frequency, band-pass filtered targets remain constant until the velocity of motion exceeds a temporal frequency of 25 Hz [19]. The results from all of these studies are consistent with the notion of a shift in spatial scale—that the sensitivity of the visual system shifts toward low spatial frequencies because high-spatial frequency components in the stimulus become 'invisible' when their motion exceeds a temporal-frequency limit.

Although there is general consensus that the shift in spatial scale of analysis is the major factor accounting for the elevation of spatial thresholds with moving stimuli, direct and supporting evidence for this hypothesis comes solely from one study [6] which examined Vernier discrimination only for stimulus velocities up to 4°/s and for stimuli that were of relatively low contrast. One purpose of this study was to provide additional evidence for the shift-in-spatial-scale hypothesis by extending the range of stimulus velocities and stimulus contrast to higher values. We also tested the hypothesis using a second spatial task, letter resolution (Experiment 2), in addition to Vernier discrimination (Experiment 1). To determine the spatial-frequency mechanisms that mediate these tasks at each velocity, we measured Vernier and letter acuities for stimuli with varying amounts of low-pass filtering and subjected the results to an equivalent blur analysis. The rationale for the low-pass filtering paradigm is that by progressively filtering out 'high' spatial-frequency components from the stimulus, we can determine the point at which the threshold for Vernier discrimination or letter resolution shifts from being limited by the *intrinsic* blur of the spatial-frequency mechanism that mediates the task to being limited by the *extrinsic* blur produced by low-pass filtering of the stimuli. Our prediction was that slowly moving stimuli would be more susceptible to the degrading effect of low-pass filtering, and that the corresponding threshold elevations would be proportional to the amount of high spatial-frequency information that is removed from the stimuli. On the other hand, because fast-moving stimuli are presumed to be analyzed primarily by low spatial-frequency mechanisms, thresholds for these stimuli were expected to survive a greater amount of low-pass filtering (i.e. a bigger loss of high spatial-frequency information) before being degraded.

2. General Methods

2.1. Visual display and experimental set-up

Stimuli for Vernier discrimination (Experiment 1) and letter resolution (Experiment 2) were presented on a Tektronix 608 oscilloscope. The oscilloscope was equipped with a P31 phosphor which has a peak luminance output at about 525 nm and a bandwidth between 75 and 125 nm. The luminance of an intensified spot diminishes to $< 1\%$ in about 250 μs, and decays more slowly thereafter. Voltage signals to the x-, y- and z-inputs of the oscilloscope were generated using a 12-bit Scientific Solutions DADIO board (Solon, OH), under the control of a 486 PC. The voltage signals were updated every 2.19 ms (frame rate = 456 Hz), as measured with a separate digitizing storage oscilloscope (Hewlett Packard 54200A). The timing of stimulus generation and synchronization of mirror movement (see below) was checked regularly during the course of data collection. Placed at a viewing distance of 3 m, both the horizontal and vertical dimensions of each dot ('pixel') on the oscilloscope were calculated to be 3.6 arc s, but the point-spread function of the dot was such that its full-width at half-height subtended 0.35 arc min, which is the dimension that we used as the width of the stimulus lines.

To reduce the effect of persistence that could result from the slow decay of phosphor after the initial 250 μs, the stimuli were superimposed on a uniform background of 50 cd/m^2 using a beam-splitter of 50% reflectance and transmittance. Uniform background luminance was provided by a diffusing plate, mounted on the exit port of an integrating chamber that was illuminated by incandescent light via a fiber optic (see Fig. 1). The beam-splitter was mounted between 7 and 8 cm in front of the observer's right (viewing) eye, with the galvanometer-mounted mirror used to produce stimulus motion closely behind. Consequently, the beam-splitter limited the size of the background field to about $32 \times 26°$ at the observer's eye. Testing was performed using the natural pupil and the non-viewing left eye was covered.

Stimulus motion was produced by the horizontal rotation of a front-surfaced mirror, mounted on a galvanometer (General Scanning G300). This galvanometer was driven by input signals from a programmable function generator (Hewlett Packard 3318A) controlled by a PET 4032 computer which was,

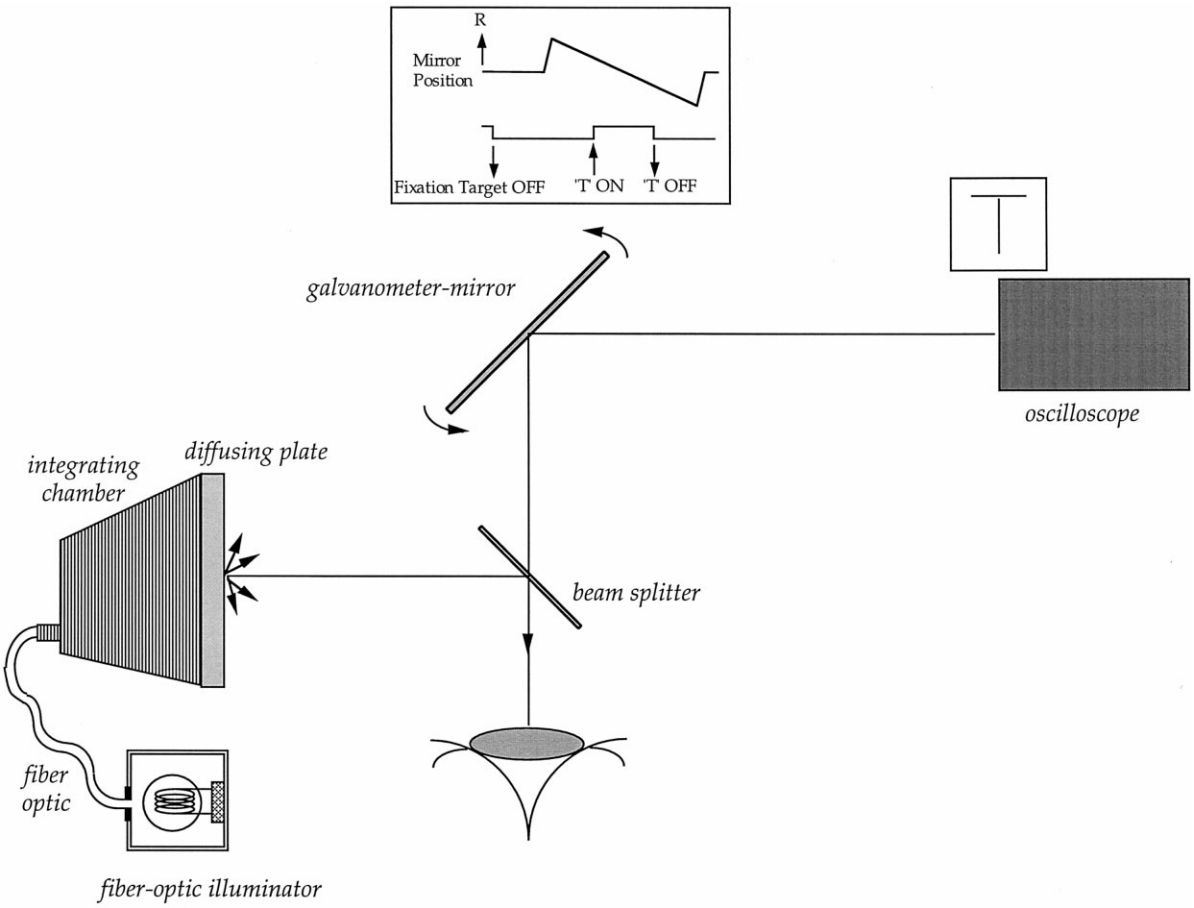

Fig. 1. Schematic diagram of the experimental set-up. The inset above the galvanometer-mirror shows one cycle of the ramp waveform of the mirror motion. The stimulus (a letter T is used in this diagram) was presented for 150 ms during the middle portion of the ramp waveform.

in turn, synchronized with the main PC used for collecting data. We used an asymmetric (10% symmetry) triangular waveform of 2.5 Hz to drive the galvanometer-mounted mirror. During each trial and upon triggering by the PC, the function generator initiated a one-cycle deflection of the mirror, randomly in the rightward or leftward direction as pre-determined by the PET computer. Stimuli were presented for 150 ms during the middle portion of the long ramp segment of the triangular waveform, which spanned a total duration of 360 ms (see Fig. 1). Consequently, any transients associated with reversals in mirror direction did not disturb the quality of the image motion. In addition, the superimposed bright background masked any visible contours so that the observer perceived a smooth sweep of the stimulus across a stationary bright field. For each velocity that we examined (0, 1, 2, 4, 6, 8 and 12°/s), a voltage signal was produced by the function generator to deflect the mirror by an appropriate amplitude.

2.2. Testing procedures

We measured thresholds for Vernier discrimination and letter resolution without and with low-pass filtering to attenuate the 'high' spatial-frequency content within the stimulus. Because both Vernier and letter acuities are contrast dependent (e.g. [20–22]), we presented the Vernier and letter stimuli at a constant visibility of 20 times above the detection threshold so that our results would not be contaminated by the reduced stimulus visibility resulting from image motion. This paradigm required us to measure the detection threshold for each testing condition before collecting data for the Vernier discrimination or letter resolution tasks. For heuristic reasons, the experiments on Vernier discrimination and letter resolution are presented in sequence in this paper, but for practical reasons, these two experiments were in fact, conducted in parallel.

Despite some subtle differences among the experiments on detection, Vernier discrimination and letter

resolution, the general procedure for a test-trial was identical. The observer, with his/her head restrained by a head rest and chin cup, was directed to look straight-ahead at a bright stationary fixation target produced on the oscilloscope. When he/she was ready, the observer pressed the fire-button on a joystick to initiate a trial which immediately turned off the fixation target. After a latency of 250 ms, the stimulus was presented on the oscilloscope for 150 ms, a duration short enough to minimize pursuit eye movements. Following the offset of the stimulus and after the mirror ceased its deflection, the observer was required to indicate his/her response for the trial, by pushing the joystick in the appropriate direction. The stationary fixation target reappeared as soon as the observer made a response.

2.3. Low-pass filtering

We low-pass filtered the stimulus by placing a diffusive glass screen in front of the oscilloscope [23,24]. This square glass screen was taller than the height of the oscilloscope screen and, therefore, did not truncate the stimulus presented on the oscilloscope. By increasing the screen-to-oscilloscope distance, progressively more 'high' spatial-frequency components were attenuated from the stimulus. In addition to attenuating high spatial-frequency components, the diffusive glass screen also reduced the maximum luminance of the stimulus. The resulting reduction in stimulus contrast was compensated by using stimuli that were normalized to the detection threshold. To calibrate the attenuation of spatial frequencies by the glass screen, we placed the glass screen at 0, 1, 3.5, 5 and 7.5 cm in front of the oscilloscope and measured the luminance profile of a line stimulus of a fixed contrast. We then Fourier transformed the spatial luminance profile into amplitudes for the various spatial-frequency components within the stimulus. Fig. 2 shows the modulation transfer of the diffusive screen for the five screen-to-oscilloscope distances. Each curve was fitted with an exponential function. We specified the cut-off spatial-frequency of these low-pass filtered images by the spatial frequency at which the amplitude drops to 1/e of the maximum value. Note that our definition of the cut-off spatial frequency, in fact, represents the bandwidth of the exponential low-pass filters [24,25]. For the five screen-to-oscilloscope distances, the corresponding cut-off frequencies are 17.1, 8.2, 3.35, 2.78 and 1.67 c/deg, respectively.

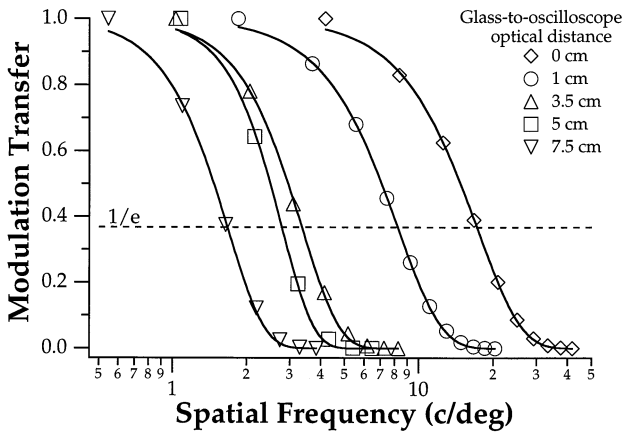

Fig. 2. Modulation transfer functions of the five low-pass filters used in this study. Normalized amplitudes of modulation are plotted as a function of spatial-frequency, determined by Fourier analysis of the line-spread function. The filters are specified in terms of the cut-off frequency (or, the bandwidth), defined as the spatial frequency at which the amplitude drops to 1/e of the maximum value. According to this criterion, cut-off frequencies for the five low-pass filters are 17.1, 8.2, 3.35, 2.78 and 1.67 c/deg, respectively.

2.4. Fixation target

For the two lowest levels of low-pass filtering (cut-off spatial frequency = 17.1 and 8.2 c/deg) and the unfiltered control conditions, the fixation target was the outline of a $0.2 \times 0.2°$ square generated and centered on the oscilloscope. For testing with the higher levels of low-pass filtering (cut-off spatial frequency = 3.35, 2.78 and 1.67 c/deg), we used fine black tape (width *ca.* 2.2 arc min) to mark the outline of a $1.4 \times 1.4°$ square on the diffusive glass-screen, and back-illuminated this black square with the outline of a square of similar size generated on the oscilloscope. Because of the diffusive properties of the glass-screen, light coming from the oscilloscope-generated square was spread out and thus acted as a source of retro-illumination. We used a large square on the diffusive glass screen to ensure that the black tape outlining the square would not interfere with the stimuli for detection, Vernier discrimination or letter resolution. For both fixation targets, we asked our observers to fixate at the center of the square and make sure that the outline was clear and sharp before initiating a trial.

2.5. Detection

Detection thresholds were measured prior to those for Vernier discrimination and letter resolution, using a staircase procedure with a two-alternative temporal forced-choice paradigm. The staircase tracked the 75% observed correct probability on the psychometric function (equivalent to 50% correct probability, after correction for guessing). This is a 2.41 down -1 up staircase, i.e. after two consecutive correct responses, there is on average a 41% chance that a third trial will be presented on which the observer must respond correctly before the contrast of the line decreases. Five reversals were determined for each staircase and the average value for the last four reversals represents the

detection threshold for that block of trials. The stimulus for the detection task was a single line of width 0.35 arc min and length 0.85°, identical to one of the pair of lines that made up the Vernier stimulus. We also normalized the T stimuli for letter resolution to the detection threshold obtained with this single line, because presumably, the Ts could be detected as soon as one of the lines is detected. For the smallest size of T used, the length of each line making up the letter was still longer than the Ricco's diameter for detecting moving objects [26], thus justifying our use of a detection stimulus that is longer than the line-lengths of the T stimuli. The contrast of the line was changed by varying the z-input to the oscilloscope, calibrated using a Pritchard Spectra-Photometer (model 1980B, Burbank, CA) with a microscanner attachment.

The starting z-value of the line stimulus was randomly selected from a set of ten possible values, all of which were above the detection threshold. On each trial, the line stimulus was presented in one of two 150-ms temporal intervals, each denoted by an audiotone. The observer's task was to indicate in which interval the stimulus was presented by pushing a joystick in one of two directions. No feedback was provided for the detection task.

2.6. Observers

Three observers, one of the authors and two observers unaware of the purpose of the study, participated in the experiments. Observers SC and TN are myopic and wore appropriate refractive correction during testing; observer KN is emmetropic. All have (corrected) vision of 20/20 or better. Observers SC and KN had prior experience in other psychophysical experiments while TN had no prior experience. Regardless of experience, all observers received extensive training with the psychophysical tasks involved and with viewing the moving stimuli. Data reported in this paper were collected only after the observers demonstrated stable thresholds for each task. Each observer voluntarily granted written informed consent after the procedures of the experiments were explained, and before the commencement of the practice sessions.

2.7. Data analyses and curve-fitting

Each datum reported in this paper represents the value averaged across four to six blocks of trials, weighted by the inverse variance of each threshold estimate [27]. Curve fitting, when necessary, was accomplished using Igor Pro™, which utilizes a Levenberg-Marquardt iterative algorithm to minimize the error between the experimental data and the model fit. Except where specified, the experimental data were weighted by the inverse of the standard error of each average threshold estimate during curve-fitting.

3. Experiment 1: Vernier discrimination

3.1. Methods

Vernier thresholds were measured for a pair of abutting vertical thin lines as a function of stimulus velocity ranging between 0 (stationary) and 12°/s, without and with one of the five levels of low-pass filtering. The dimensions of the abutting lines were 0.35 arc min by 0.85°. This line-length was long enough to attain optimal Vernier acuity even for the highest velocity that we examined, as determined from a pilot experiment. Vernier offset was introduced by horizontally shifting the upper test line relative to the lower reference line. We presented the stimulus using the method of constant stimuli where, within each block of 70 trials, the upper test line was presented at one of seven offset positions: 1, 2 or 3 units to the right or left of the lower reference line, or aligned with it. The order of presentation was randomized. The task of the observer was to discriminate the relative position of the upper line with respect to the lower one, by pushing a joystick toward the right or left. Audio feedback indicated whether or not the observer's response to the previous trial was correct. Responses to the 'right' were tallied for each block of trials. We analyzed the data using probit analysis where Vernier threshold was defined as the range of offsets corresponding to a change from 50 to 84% rightward responses on the psychometric function, equivalent to 1 S.D. of the cumulative Gaussian distribution of the responses.

3.2. Results

Vernier thresholds obtained for the five levels of low-pass filtering, and the unfiltered control condition, are plotted as a function of stimulus velocity in Fig. 3. For the unfiltered control condition (smallest unfilled symbols in each panel), Vernier threshold worsens with image motion, even though the stimuli were equally visible. This result is similar to and extends that of our earlier study [6], in which we showed that Vernier thresholds for broad-band stimuli that are three or four times the detection threshold increase monotonically from 0 to 6°/s. Here, we demonstrate that this effect applies to stimuli that are more visible (20 times the detection threshold) and move faster (up to 12°/s). In addition, because of the higher visibility of the stimuli used in the present study, our data show the well-known robustness of Vernier thresholds to low velocities of motion [1,28]. Specifically, image motion was tolerated without degradation of the Vernier threshold up to 1°/s for observer SC and 2°/s for observer KN. Observer TN did not show a tolerance to image motion for the unfiltered control condition. We attribute the differential tolerance of Vernier thresholds to slow im-

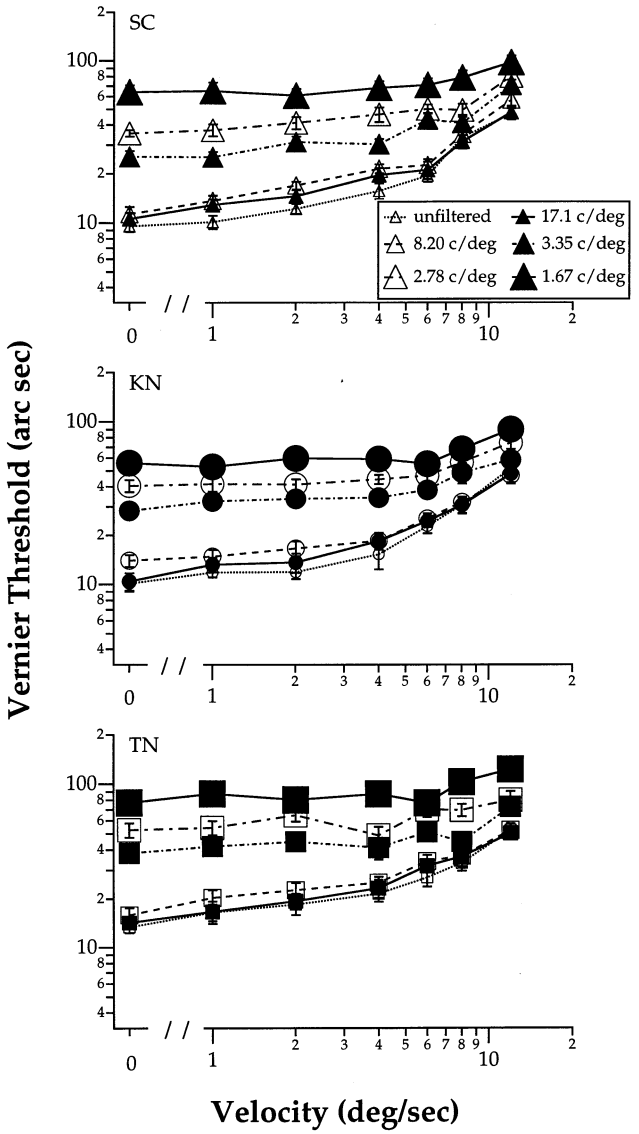

Fig. 3. Vernier threshold (arc s) is plotted as a function of velocity (°/s), without (smallest unfilled symbols in each panel) and with (larger filled and unfilled symbols) low-pass filtering. The size of the symbols codes the amount of high spatial-frequency attenuation (see legend in the top panel, which applies also to the other panels except for the shape of the symbols). Each panel gives the data for one observer. Note that Vernier threshold shows a higher tolerance to stimulus velocity when the stimuli are low-pass filtered. Error bars represent ± 1 S.E.M., and are smaller than the size of the symbol when not shown.

age motion to the idiosyncrasies of the individual observers.

With low-pass filtering, Vernier thresholds generally worsen as the cut-off frequency of the filter is reduced. However, this effect is velocity-dependent, as seen from the more prominent degradation of Vernier thresholds by low-pass spatial filtering at low than at high stimulus velocities. For an increase in stimulus velocity from 0 to 12°/s, Vernier threshold increases by an average factor of 4.67 without filtering, compared to a factor of only 1.58 with the highest level of low-pass filtering (cut-off spatial frequency = 1.67 c/deg). In other words, Vernier threshold shows a higher tolerance to image motion when the high spatial-frequency components of the stimulus are attenuated. Fig. 3 shows that Vernier thresholds remain more or less constant for velocities up to about 6°/s with the highest level of filtering, compared to only 1 or 2°/s for the unfiltered control condition.

To examine more closely the effect of spatial-frequency content of the stimulus on Vernier thresholds, we replotted the data in Fig. 3 as a function of the spatial period of the cut-off spatial frequency of the different low-pass filters, for the seven stimulus velocities that we tested (Fig. 4). For comparison, thresholds obtained with the unfiltered control condition are shown in Fig. 4 as the isolated symbols plotted close to the ordinate.

We fitted the data-set for each stimulus velocity in Fig. 4 with the following equation (velocity coded by the size of symbols):

$$\text{Threshold} = \text{Th}_{\text{unfiltered}} \times \sqrt{1 + \left(\frac{\text{spatial period of filter}}{b_i}\right)^2} \quad (1)$$

where $\text{Th}_{\text{unfiltered}}$ represents the optimal unfiltered Vernier threshold at the specific stimulus velocity, and b_i represents an estimate of the 'equivalent intrinsic blur' present in the visual system. This equation is similar to that used by previous researchers to analyze the amount of intrinsic noise or blur in the visual system (e.g. [29–34]). In these previous studies, the rationale for fitting this equation was that the visual system itself possesses a certain level of intrinsic noise or blur, which limits visual performance until exceeded by externally imposed noise or blur. Hence, the magnitude of the extrinsic noise at which visual performance starts to be degraded can be taken as an estimate of the intrinsic noise of the visual system. Following the argument by Levi and Klein [33] that intrinsic blur may result from the optics of the eye as well as the discrete sampling by the photoreceptors, we will use their term, 'equivalent intrinsic blur', to represent the intrinsic factor that limits visual performance. Note that the term equivalent intrinsic blur is applicable to any source of blur that is additive to the extrinsic blur imposed upon the stimulus (D.M. Levi, personal communication). With respect to our experiment, the change in the equivalent intrinsic blur can be a consequence of either a change in the retinal area that is stimulated by the motion smear, or a shift in sensitivity of the visual system toward lower (thus, larger in spatial scale) spatial-frequency mechanisms. Based on our previous finding [6], we assume for now that the change in the equivalent intrinsic blur is due primarily

to a shift in the spatial scale in analysis. This issue will be further addressed in Section 6.

Based upon the logic presented above, we conducted an equivalent blur analysis to determine if the equivalent intrinsic blur of the visual system increases when analyzing moving stimuli. Previous researchers suggested that the intrinsic 'blur' of a spatial-frequency mechanism is proportional to its size [14,15]; here, we further assumed that we can represent the intrinsic blur of a spatial-frequency mechanism by its spatial size. Curve-fitting was performed on data obtained with low-pass filtered stimuli, with the optimal threshold constrained to the value measured for the unfiltered condition at each velocity. For each velocity, the estimated equivalent intrinsic blur (b_i) obtained from the best-fit equation is displayed just above the abscissa in each panel of Fig. 4 and summarized in Table 1. The progressive increase in symbol size rightward on the abscissa indicates that the estimated equivalent intrinsic blur increases with stimulus velocity (repeated measures ANOVA: $F_{(df=6,20)} = 35.6,\ P < 0.0001$).

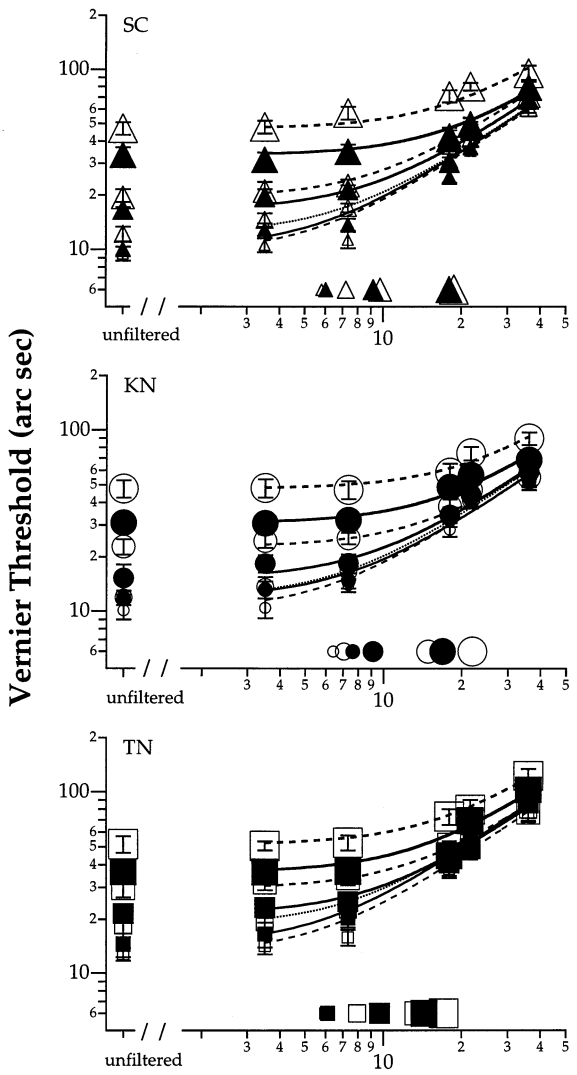

Fig. 4. Vernier threshold (arc s) is plotted as a function of the spatial period of the cut-off frequency of each low-pass filter (arc min). The stacks of datum points plotted close to the ordinate represent thresholds obtained without low-pass filtering (velocities are coded by the size of individual symbols: smallest = 0°/s; largest = 12°/s). Data connected by lines are thresholds obtained with different levels of low-pass filtering. Lines represent the fitted equivalent blur equation (see text for details) used to estimate the equivalent intrinsic blur. The equivalent intrinsic blur estimates are represented by the row of datum points lying just above the abscissa. Error bars represent ± 1 S.E.M.

3.3. Discussion

Vernier thresholds are elevated but are more tolerant of image motion when the stimuli are low-pass filtered. That is, the stimulus velocity at which Vernier thresholds start to increase is higher when the stimulus is restricted to low spatial-frequency components, and lower when the stimulus contains more high spatial-frequency components. These results can be understood in terms of the spatial-frequency content of the stimulus in the presence of image motion or low-pass spatial-filtering. When a stimulus moves, the mechanism that mediates the task is hypothesized to shift toward lower spatial frequencies [6]. For an unfiltered stimulus that possesses high spatial-frequency components, this shift in spatial scale will cause an elevation in Vernier threshold, which is proportional to the shift in spatial-scale ([6], also see below). In contrast, a low-pass filtered stimulus lacks high spatial-frequency components; thus, a shift in spatial-scale will not occur until the stimulus velocity is high enough to require an even-lower frequency mechanism to mediate the task.

Our results confirm that 'high' spatial frequencies are important in mediating optimal Vernier discrimination. At 0 and 1°/s, our estimates of the equivalent intrinsic blur suggest that a spatial-frequency mechanism with a spatial period of about 6–6.6 arc min (corresponding to spatial frequencies of about 10–9.1 c/deg) are most important in mediating Vernier discrimination. At 12°/s, our analysis implies that a spatial-frequency mechanism with a spatial period of about 19 arc min (spatial frequency = 3.1 c/deg) mediates Vernier thresholds. Note that the crucial spatial frequency for stationary stimuli as estimated using the equivalent blur analysis is very similar to that obtained using a masking paradigm [6,35]. The progressive increase in the equivalent intrinsic blur when velocity increases from 0 to 12°/s suggests that the size of the spatial-frequency mechanism underlying Vernier discrimination increases with stimulus velocity.

To quantitatively relate Vernier thresholds to the size of the spatial-frequency mechanisms that are inferred to mediate the task, we plotted *unfiltered* Vernier

Table 1
Equivalent intrinsic blur (unit: arc min) estimated for Vernier discrimination and letter resolution

Velocity (°/s)	Vernier discrimination				Letter resolution			
	SC	KN	TN	Average	SC	KN	TN	Average
0	5.79 ± 0.28	6.40 ± 0.24	5.96 ± 0.19	6.05 ± 0.23	6.34 ± 0.18	4.12 ± 0.14	5.42 ± 0.13	5.29 ± 0.65
1	6.00 ± 0.29	7.60 ± 0.39	6.11 ± 0.10	6.57 ± 0.54	7.42 ± 0.31	4.74 ± 0.12	6.54 ± 0.21	6.23 ± 0.80
2	7.19 ± 0.15	7.03 ± 0.16	7.92 ± 0.45	7.38 ± 0.32	7.81 ± 0.28	5.19 ± 0.20	6.92 ± 0.16	6.64 ± 0.78
4	9.15 ± 0.39	9.10 ± 0.36	9.66 ± 0.32	9.30 ± 0.27	9.75 ± 0.38	6.15 ± 0.26	8.00 ± 0.40	7.97 ± 1.06
6	9.75 ± 0.28	14.83 ± 0.91	13.41 ± 1.06	12.66 ± 1.59	11.51 ± 0.36	7.88 ± 0.33	9.88 ± 0.37	9.76 ± 1.07
8	17.93 ± 0.93	16.85 ± 0.93	14.33 ± 0.96	16.37 ± 1.19	13.15 ± 0.49	8.76 ± 0.46	10.05 ± 0.59	10.65 ± 1.34
12	18.68 ± 1.24	21.89 ± 1.11	17.04 ± 0.37	19.21 ± 1.53	13.38 ± 0.86	9.88 ± 0.27	12.17 ± 0.47	11.81 ± 1.08

thresholds obtained at different velocities as a function of the size of the spatial-frequency mechanism as estimated from the equivalent blur analysis (Fig. 5). The straight line drawn through the data on log–log coordinates is the best-fit power function fitted to the data *without* weighting. If the change in the size of the spatial-frequency mechanism as estimated from the equivalent blur analysis perfectly predicts the change in Vernier thresholds, then this line should have a slope (i.e. exponent of the power function) of one. The slope of the fitted line is 1.18 ± 0.12 which, statistically, is not significantly different from a slope of one ($F_{(df=1,19)} = 2.32$, $P = 0.14$).

The data in Fig. 5 suggest that the equivalent intrinsic blur of the visual system at each velocity can predict the optimal Vernier threshold that can be attained. However, there is at least one aspect of our data that is quantitatively at odds with the results of our previous study using a masking paradigm [6]. Similar relationships between Vernier threshold and the size of the spatial-frequency mechanism mediating the task at different velocities yielded a slope between 0.75 and 0.80 in our previous study, which is lower than the slope that we obtained from the present experiment. One reason that could account for this difference in slope is that we examined a three-times greater range of velocity than in our earlier study, which should have provided a better representation of the relationship between Vernier threshold and size of spatial-frequency mechanism. Another factor that could account for the difference in slope is that we used higher stimulus contrast in the present experiment (20 times the detection threshold, in comparison to three or four times in our earlier study). As we argued in our earlier paper, even though we equated the broad-band Vernier stimulus for visibility, we were probably equating visibility for the lower spatial-frequency mechanisms that mediate target detection, instead of the higher spatial-frequency mechanisms that mediate Vernier discrimination [6]. Therefore, effectively, the contrast for the mechanisms that mediated Vernier discrimination was lower than the nominal value. We reasoned in this previous study that if the visibility had been equated for the mechanisms that mediated the Vernier task, then a slope closer to one would be obtained. The present experiment used stimuli that were 20 times above the detection threshold, so that the contrast-response of both low and high spatial-frequency mechanisms may have saturated or come close to saturating. Consequently, any discrepancy between the spatial-frequency mechanisms used for detection and Vernier discrimination should be small.

4. Experiment 2: Letter resolution

The results of Experiment 1, together with those from our earlier study [6], demonstrate that a shift in the spatial scale of analysis can explain the threshold

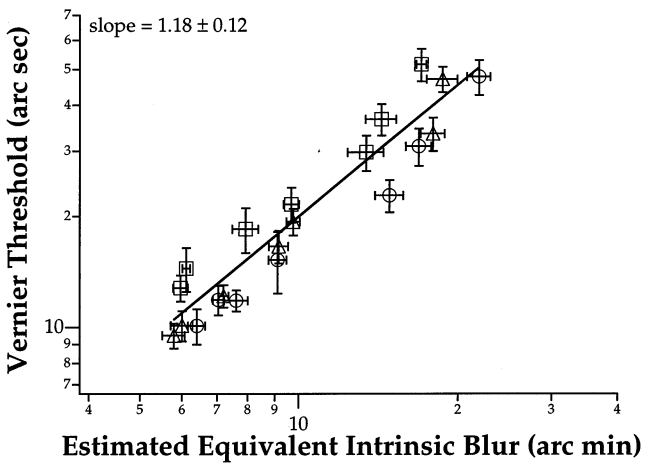

Fig. 5. Unfiltered Vernier threshold (datum points plotted close to the ordinate in Fig. 4) is plotted as a function of the estimated equivalent intrinsic blur (datum points presented close to the abscissa in Fig. 4). Here, we assume that the equivalent intrinsic blur is identical to the period of the spatial-frequency mechanism mediating the task. Data from the different observers are represented by different symbol shapes. The straight line is the best-fit power function fitted through the data *without* weighting. Vertical error bars represent ± 1 S.E.M. of Vernier thresholds and horizontal error bars represent ± 1 S.E. of estimate of the equivalent intrinsic blur.

elevation for moving Vernier stimuli. In this experiment, we asked if the same reasoning applies to another spatial task–letter resolution.

At least three major differences exist between the tasks of letter resolution and Vernier discrimination. Letter resolution is believed to be more reflective of the highest spatial-frequency mechanism that exists in the visual system than the Vernier task [36,37]. For Snellen letters, it has long been assumed that standard visual acuity is attained if the detail of a letter, subtending 1 arc min, is resolvable [38,39]. This minimum angle of resolution (MAR) when translated into spatial frequency, corresponds to 30 c/deg[1]. For Vernier discrimination, the crucial spatial-frequency mechanisms are believed to fall within 10–15 c/deg for stationary stimuli ([6,35,42], also see results above). In other words, letter resolution may be a more appropriate task to reveal the highest spatial-frequency mechanism that is present within the visual system. Nevertheless, thresholds for letter resolution (MAR) are usually around 0.5 to 1 arc min, which is about four to six times worse than those for Vernier discrimination under optimal conditions. Finally, retinal eccentricity produces differential effects on letter and Vernier acuities, suggesting that the two tasks may be limited by different mechanisms in the visual system. Specifically, the retinal eccentricities at which threshold doubles in value (E_2 factor) are about 1.5 and 0.9° for letter and Vernier acuities, respectively [12,21,43–46]. However, note that except for the study of Virsu et al. [44], these E_2 values were obtained from and compared across different groups of observers.

In view of the possibly different mechanisms underlying letter resolution and Vernier discrimination, image motion may differentially degrade these two tasks. Hence, the aim of this experiment was to determine if a shift in spatial scale can similarly explain why letter acuity is degraded in the presence of image motion.

4.1. Methods

We measured letter acuity using a letter 'T', without and with one of the five levels of low-pass filtering produced by the diffusive ground-glass screen, as in Experiment 1. Each stimulus T was made up of two thin lines of identical length [47]. We used these thin-line Ts instead of ones that conform to the conventional Snellen notation (details of the letter equal to one-fifth of the whole letter size) for two practical reasons. First, the lines comprising the thin-line T stimulus are directly comparable to the stimuli used in the detection and Vernier tasks. Second, a Snellen T takes a significantly longer time to generate on the oscilloscope, which results in too low of a 'frame rate' for stimuli presented in motion. During each trial, the letter T was presented in one of four orientations: up, down, right or left. We presented the stimulus using the method of constant stimuli where, within each block of 96 trials, six different sizes of Ts, in approximately 0.1 log unit steps, were each presented 16 times, four in each orientation. The order of presentation of each letter size and orientation was randomized. The task of the observer was to discriminate the orientation of the Ts by pushing the joystick in the corresponding direction. Audio feedback indicated whether or not the observer's response to the previous trial was correct. The observer's correct responses for each letter size and orientation for each block of trials were tallied. We analyzed the data using probit analysis where the threshold for letter resolution was defined as the letter size that gives 62.5% correct on the psychometric function (equivalent to 50% correct recognition, after correction for guessing using a four-alternative forced-choice paradigm).

Because our letter T stimuli did not conform to the conventional Snellen configuration (stroke width = 1/5 letter size), we compared acuities obtained using the line Ts and standard Landolt C stimuli in two observers. High-contrast Landolt C stimuli (stroke width = 1/5 letter size) were projected from slides onto a white matte screen at 4.1 m as white letters on a dark background. The Cs were viewed after reflection from the galvanometer-mounted mirror, and superimposed on the same background as used in the main experiment. A shutter was placed in front of the projector which, when triggered by the computer, limited the presentation time to 150 ms. Acuities for Landolt Cs were measured at the seven velocities used in the main experiment.

4.2. Results

Fig. 6 compares acuities obtained for unfiltered Ts and Landolt Cs for two observers (top and middle panels). The logMAR value plotted on the ordinate refers to the resolution for Landolt Cs, in which the detail is equivalent to one-fifth of the whole letter size. For comparison, we only used one-fifth of the whole letter size of Ts as the resolution acuity in this figure. As shown in Fig. 6, although T acuity is better than that for Landolt Cs by a factor of 2.5–3, letter acuity obtained for the two types of stimuli worsens with image motion in a similar way, as shown by the more or less parallel curves for each observer. Averaged

[1] Recently, Bondarko and Danilova [40] proposed that the resolution of foveal Landolt Cs is determined by the detection of spatial frequencies corresponding to only 1.3, rather than 2.5 cycles/letter. However, because the visual acuity of well-corrected normal observers is typically on the order of 20/15 to 20/17 [41], the spatial frequency corresponding to 1.3 cycles/letter still falls in the range of 18–21 c/deg.

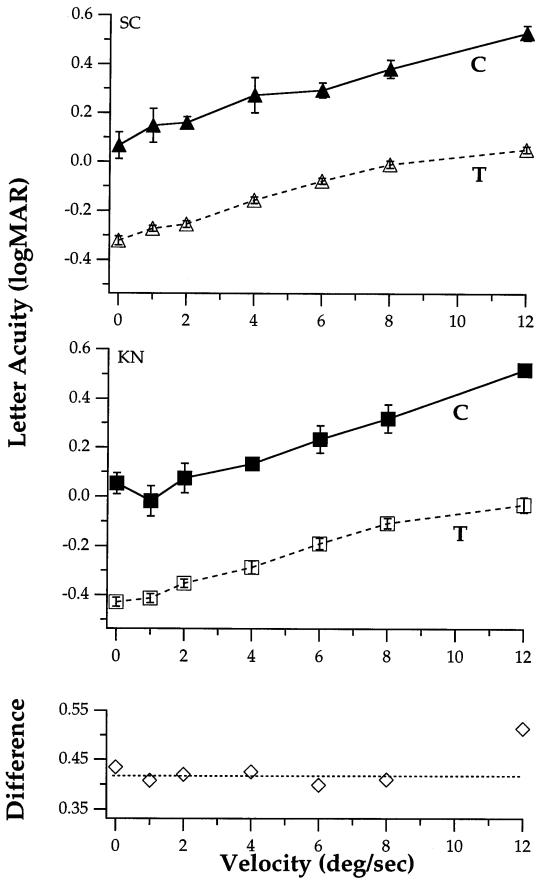

Fig. 6. Letter acuity, represented as one-fifth of the letter size and given as the logarithm of the minimum angle of resolution (logMAR), is compared for the letter T stimuli used in this study (unfilled symbols with dashed lines) and conventional Landolt C stimuli (filled symbols with solid lines) for two observers (top and middle panels), as a function of velocity. The difference in acuities for the two types of stimuli, averaged across the two observers, is given in the bottom panel where the dotted line represents a constant difference of 0.42 log units. The difference between T- and C-acuities are similar between velocities of 0 and 8°/s, but increases for a velocity of 12°/s.

across the two observers (Fig. 6: bottom panel), the difference between T- and C-acuity is similar for stimulus velocities between 0 and 8°/s, but increases by about 0.1 log units for a stimulus velocity of 12°/s. We conclude that the results obtained with the T stimuli can be generalized to other letter resolution tasks as well.

Letter resolution thresholds, measured for the five levels of low-pass filtering, together with the unfiltered control condition, are plotted as a function of velocity in Fig. 7. In Fig. 7 and in the remainder of the paper, letter acuities are expressed in terms of the *whole* letter size of the T stimuli. As expected, letter acuities worsen with image motion and, like the results obtained for Vernier targets in Experiment 1, this effect depends on the level of low-pass filtering. In other words, the deleterious effect of image motion on letter resolution depends on the spatial-frequency content of the stimulus. For the unfiltered control condition, letter acuity tolerates image motion up to about 2°/s without degradation [1,3,4,48]. Note that, like her Vernier acuity, observer TN had noticeably worse acuity for a stimulus moving at 1°/s than for a stationary stimulus. With increasing levels of low-pass spatial filtering, letter acuities are less affected by image motion, as represented by a larger range of velocity over which acuities remain more or less constant. Specifically, with an increase in stimulus velocity from 0 to 12°/s, letter acuity worsens by an average factor of 2.43 without filtering, and only 1.12 when the stimuli were subjected to the highest level of low-pass filtering (cut-off spatial frequency = 1.67 c/deg). The increased tolerance of letter acuity to motion in the presence of extrinsic blur,

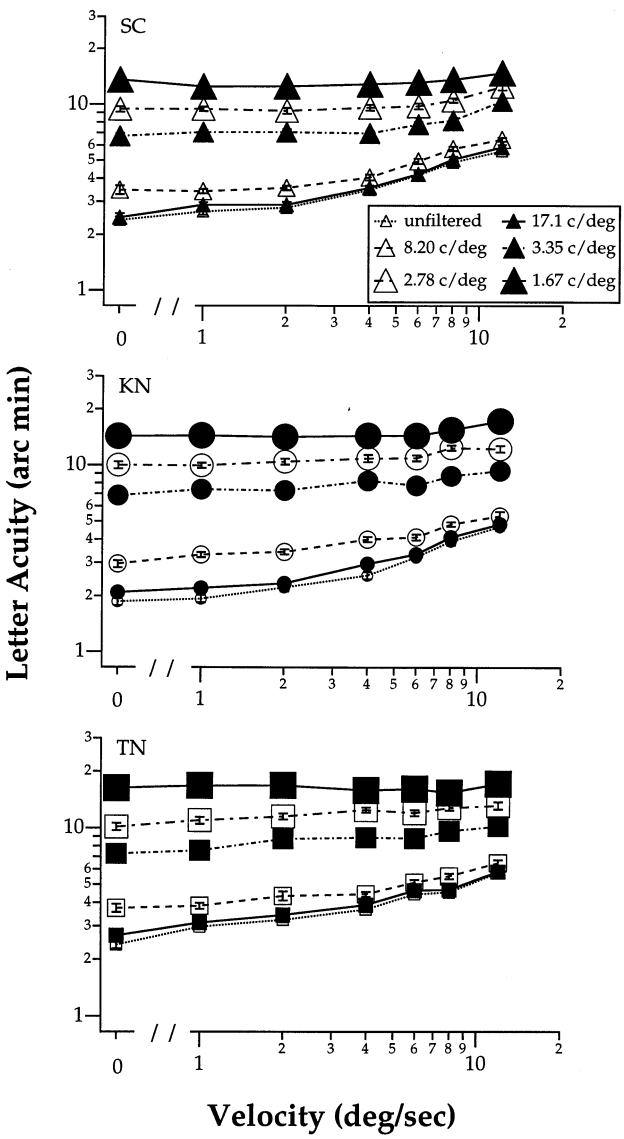

Fig. 7. Letter acuity (arc min), represented as the whole letter size of the Ts, is plotted as a function of stimulus velocity, without (smallest unfilled symbols in each panel) and with (larger filled and unfilled symbols) low-pass filtering. Details of the figure are as in Fig. 3.

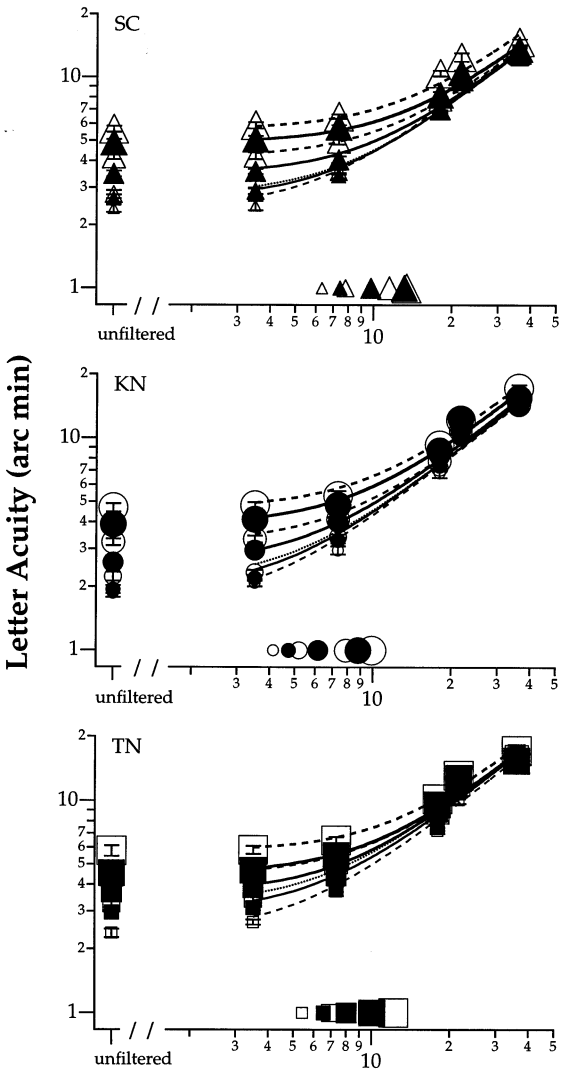

Fig. 8. Letter acuity (arc min) is plotted as a function of the spatial period of the cut-off frequency of each low-pass filter (arc min). Details of the figure are as in Fig. 4.

and the magnitude of change of acuity with velocity for physically unblurred stimuli, are consistent with the findings of an earlier study [49], despite major methodological differences in the parameters of image motion.

To determine whether a shift in spatial scale can explain the threshold elevation in letter acuity with moving stimuli, we conducted an equivalent blur analysis on our letter-acuity data. In Fig. 8, letter acuity is plotted as a function of the spatial period of the cut-off frequency for each of the five low-pass filters, as for Vernier acuity in Fig. 4. Curve fitting using Eq. (1), as described above for Experiment 1, was carried out on the data-set for each stimulus velocity, again, with the optimal acuity constrained to the value obtained without filtering. Similar to the results obtained with Vernier thresholds, the estimated equivalent intrinsic blur for letter resolution shifts toward higher values for moving stimuli, implying that mechanisms having more equivalent intrinsic blur underlie letter resolution at higher stimulus velocities. The amount of equivalent intrinsic blur estimated for the three observers, as a function of velocity, are shown in Fig. 8 and are tabulated in Table 1. Repeated measures ANOVA confirms that the intrinsic blur of the visual system increases with stimulus velocity ($F_{(df=6,20)} = 80.6$, $P < 0.0001$).

4.3. Discussion

As found for Vernier acuity, and in general agreement with previous studies [49,50], letter acuity can withstand a higher stimulus velocity in the presence of extrinsic blur before it is degraded by image motion. The highest velocity that letter acuity can tolerate without any degradation is about 2°/s for a 'blur-free' stimulus, which is in good agreement with that reported by Brown [3] and Westheimer and McKee [1]. With the highest level of low-pass filtering that we used (cut-off frequency = 1.67 c/deg), acuities could survive image motion of up to at least 8°/s. The increased tolerance to image motion when acuity is already degraded is analogous to the increased tolerance to optical blur in patients who have impaired vision [51].

The progressive increase in the intrinsic blur of the spatial-frequency mechanism used to analyze moving letters suggests that the size of the spatial-frequency mechanism underlying the letter-acuity task increases with stimulus velocity. To quantify the relationship between letter acuity and the size of the spatial-frequency mechanism used, we again fit a power function relating letter acuity to the estimated intrinsic blur at each velocity. These data are plotted in Fig. 9, where the line represents the power function fitted to the datum points *without* weighting. The slope of this line is 0.98, which clearly does not differ from a slope of one ($F_{(df=1,19)} = 0.075$, $P = 0.79$).

5. Control experiment: Effect of retinal eccentricity

Although it is accepted that the elevation in spatial thresholds for moving stimuli is due primarily to the image motion *per se*, and not the fact that stimuli are presented at extrafoveal locations, direct and quantitative comparisons are scarce. Ludvigh [2] compared acuity measurements obtained with circular image motion to data from another study that examined visual acuity as a function of eccentric retinal position [52]. However, the measurements being compared were not made on the same observers nor were they obtained under identical testing conditions. Morgan et al. [5] directly compared Vernier thresholds for stimuli that

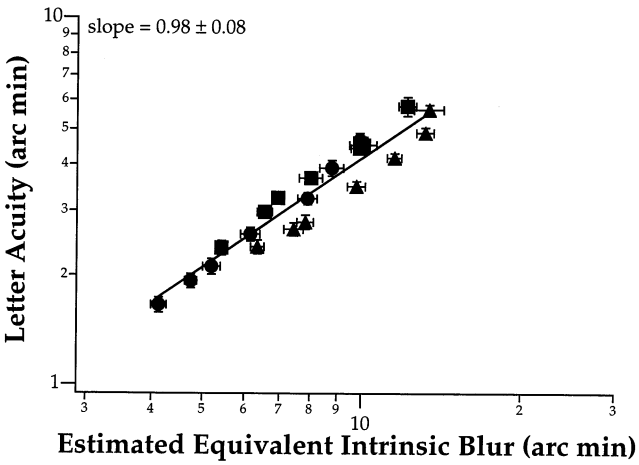

Fig. 9. Letter acuity obtained without low-pass filtering (datum points plotted close to the ordinate in Fig. 8) is plotted as a function of the estimated equivalent intrinsic blur (datum points presented close to the abscissa in Fig. 8). Details of the figure are as in Fig. 5. The straight line represents the best-fit power function fitted to the data *without* weighting.

moved at 3°/s for repetitive brief exposures (each < 250 ms) to thresholds obtained with stationary stimuli exposed for 250 ms at the eccentric retinal location corresponding to the end-point of the motion trajectory for each moving-stimulus exposure duration. Their data convincingly show that the elevation of Vernier threshold attributable to retinal eccentricity could not fully explain the degradation arising from retinal image motion. However, because they presented their moving stimuli repetitively until the observer responded, the thresholds that they obtained may have been influenced by probability summation across multiple glimpses of the stimuli. Hence, the purpose of this control experiment was to quantify the relative contribution of eccentricity in elevating the threshold for moving stimuli, for both Vernier discrimination and letter resolution.

5.1. Methods

We compared thresholds for Vernier discrimination and letter resolution for stimulus velocities of 6 and 12°/s to thresholds measured with stationary stimuli placed at retinal locations that correspond to the end-points of these motion trajectories. For a stimulus duration of 150 ms, these end-points correspond to 0.45 and 0.9°, for stimulus velocities of 6 and 12°/s, respectively. Data were collected using identical stimulus configurations and psychophysical procedures as those described in Experiments 1 and 2, with the exception that the moving stimulus was replaced by a stationary one presented randomly to the right or left of the location previously occupied by the center of the fixation target. Unfiltered stimuli were used in this control experiment. The visibility of each stimulus was set to be 20 times above the detection threshold, as in the main experiments.

5.2. Results

Thresholds obtained with stationary stimuli placed at 0.45 and 0.9° from the fovea were normalized to each observer's threshold obtained for the foveally presented, stationary stimuli. The normalized thresholds

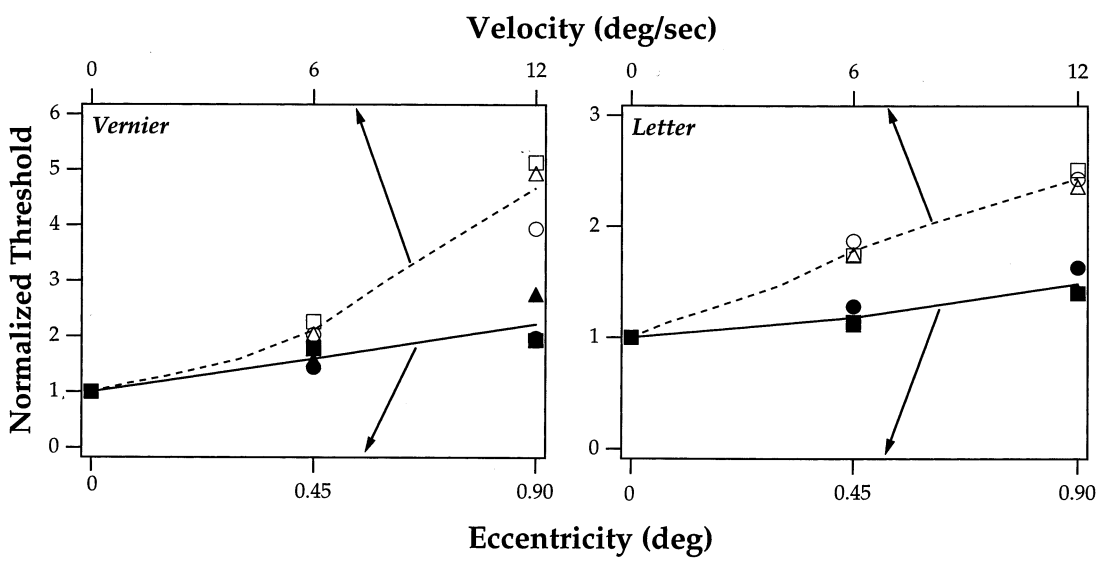

Fig. 10. Normalized thresholds for Vernier discrimination (left) and letter resolution (right), averaged across the three observers, are plotted as a function of the retinal eccentricity of a stationary stimulus (bottom axes: filled symbols and solid lines) that corresponds to the end-point of the motion trajectory for selected moving stimuli. For comparison, the normalized thresholds for moving stimuli are also given (top axes: unfilled symbols and dashed lines). Dashed lines connect the averaged normalized thresholds for the seven velocities used, but datum points are only plotted for velocities of 0, 6 and 12°/s. Note the 2-fold change in scale of ordinate between the left and right panels.

are presented as a function of retinal eccentricity (filled symbols) in Fig. 10, for both Vernier discrimination (left) and letter resolution (right). For comparison, we also included normalized thresholds obtained for stimuli moving at 6 and 12°/s (unfilled symbols). Clearly, thresholds obtained with extrafoveally presented stationary stimuli are better than those obtained with moving stimuli. From these data, the estimated E_2 factor for Vernier discrimination is approximately 0.9°; while the extrapolated E_2 value for letter resolution is about 2.2°. The E_2 value for Vernier discrimination is in good agreement with those reported in the literature (e.g. [12,43,45,46]), but that for letter resolution is higher than most reported values ($\cong 1.5$ for letter resolution [21]). This difference in the E_2 values for letter resolution may be a consequence of extrapolating from only three datum points, all of which are obtained at relatively small eccentricities.

5.3. Discussion

By comparing thresholds for moving *versus* stationary stimuli placed at an eccentricity corresponding to the end-point of the motion trajectory, we demonstrated that although retinal eccentricity has a degrading effect on Vernier and letter acuities, the effect is small compared to the overall effect of image motion. Note that our use of eccentricities corresponding to the end-points of the motion trajectory probably overestimates the real contribution of eccentricity, which might be better approximated as half of the maximum eccentricity of the trajectory. In other words, the actual magnitude of effect attributable to eccentricity may be even smaller than that presented in Fig. 10. Another conclusion that can be drawn from the data in Fig. 10 is that both eccentricity and image motion have different effects on Vernier discrimination and letter resolution. Specifically, Vernier discrimination is more susceptible to degradation by both the eccentric positioning of the stimulus and image motion, compared to letter resolution. Considering that both eccentricity and image motion call for a shift in the spatial scale in analyzing the stimulus, the similarity in the differential degrading effect of these two effects on Vernier and letter acuities is not surprising.

6. General discussion

6.1. Intrinsic versus extrinsic blur

In this study, we utilized equivalent blur analysis as a tool to infer whether a shift in spatial scale occurs when the visual system analyzes moving stimuli. Results from Experiments 1 and 2 both demonstrate that the estimated equivalent intrinsic blur increases in parallel with the stimulus velocity, at least for velocities ranging between 0 and 12°/s. We infer from these findings that progressively larger (and thus lower) spatial-frequency mechanisms are used when the stimulus velocity increases from 0 to 12°/s. However, is this inference valid? We previously showed that identical Landolt C acuity was obtained for image motion up to 16°/s, as long as the extent of retinal stimulation by motion smear was equated within the temporal integration period for complete summation. This finding suggests that the increase in the equivalent intrinsic blur may be related to the extent of motion smear, rather than velocity *per se*. If this argument is correct, then the two sources of blur that entered into our equivalent blur analyses would be the extrinsic blur provided by the low-pass filtering of the stimulus, and the blur produced by the extent of the motion smear on the retina.

Table 1 shows that the equivalent intrinsic blur estimates, averaged across the three observers, increase by a factor of about 3.18 for Vernier discrimination, compared to a factor of only 2.23 for letter resolution, as stimulus velocity increased from 0 to 12°/s. This differential change in the equivalent intrinsic blur for the two tasks suggests that the extent of motion smear does not, by itself, account for the change in the equivalent intrinsic blur with stimulus velocity. Instead, we conclude that the retinal extent of stimulation is the trigger for a shift in spatial scale, and that performance depends ultimately upon the spatio-temporal frequency characteristics of the mechanisms used to perform a specific task.

6.2. Spatio-temporal limitations

Substantial psychophysical and neurophysiological data support the idea that pattern vision in the human and primate visual systems is analyzed by 'channels', i.e. parallel pathways that are most sensitive to certain spatial-frequency bands within a stimulus and thus respond optimally to them (e.g. [7,42,53–58]). The sensitivity of these channels has been shown to depend on *both* the spatial and temporal frequencies of the stimulus [7,59]. For stationary targets, Vernier thresholds have been shown to be determined by the slope of the spatial tuning function of the operating mechanism, i.e. the change in sensitivity of the mechanism with position. Consequently, as long as the same amount of stimulus energy is available, a low frequency mechanism with a flatter slope will yield a lower sensitivity (thus a higher threshold) than a high-frequency mechanism with a steeper slope [12–16].

Considering that these spatio-temporal frequency mechanisms are contrast-dependent, such that better responses are obtained with higher stimulus contrast, spatial thresholds may indeed be governed by the spatial contrast gradient of the optimally responding mech-

anism. We define the spatial contrast gradient as the product of the slope of the operating spatial mechanism and the available stimulus contrast energy. If this argument is correct, then a high spatial-frequency stimulus of low contrast should yield the same threshold as a low spatial-frequency stimulus of high contrast, because of identical spatial contrast gradients. This trade-off between stimulus spatial frequency and contrast stands only if (i) sensitivity to the task increases directly and proportionally with the stimulus contrast; and (ii) task performance is proportional to the size of the operating spatial mechanism. Vernier acuity for stationary abutting targets is highly contrast dependent (e.g. [6,22,46]) and can be predicted from the size of the operating spatial-frequency mechanism ([6], see also Fig. 5). For comparison, thresholds for moving Vernier targets also improve with contrast, at least up to several times the detection threshold [6,18], suggesting a contrast dependence similar to that for stationary targets.

We propose that the limiting factors for analyzing moving targets—spatial frequency, temporal frequency and contrast, are all tied to, and represent different facets of the spatio-temporal response properties of the visual system. Consequently, over a wide range, acuity for abutting Vernier targets depends on the spatial contrast gradient. Although letter acuity also depends on the size of the operating spatial-frequency mechanism (Fig. 9), it is less contrast dependent than Vernier acuity [20,21,60,61]. Thus, letter resolution does not vary proportionally with the spatial contrast gradient. This differential contrast dependence for Vernier and letter acuities suggests that spatial thresholds for moving targets do not depend solely on the spatio-temporal frequency and contrast of the stimuli. Rather, these thresholds depend upon the combination of the spatio-temporal energy available in the stimulus and the response properties of the responding neural mechanisms.

6.3. Vernier discrimination versus letter resolution

As summarized in the Introduction to Experiment 2, evidence exists to suggest that the underlying mechanisms for Vernier discrimination and letter resolution may be different. A comparison of our data for the two tasks, obtained from the same observers, confirms that indeed, visual performance is affected differently by stimulus velocity, extrinsic blur, and retinal eccentricity. With an increase in stimulus velocity from 0 to 12°/s, Vernier thresholds for unfiltered stimuli increase by a factor of 4.67 while those for letter resolution increase by only a factor of 2.43. For stimuli with the maximum amount of low-pass filtering, these changes in threshold diminish to factors of 1.58 and 1.12 for Vernier discrimination and letter resolution, respectively. And, for stationary stimuli, the E_2 factors as estimated from our control experiment are about 0.9 and 2.2° for Vernier

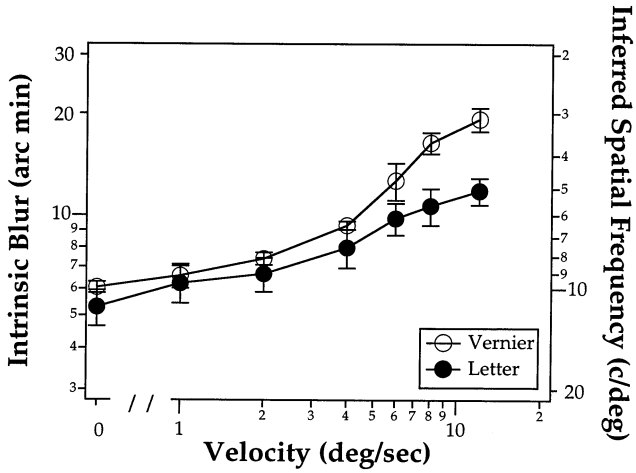

Fig. 11. Estimated intrinsic blur (left ordinate: arc min) and the tuning of the corresponding inferred spatial frequency mechanism (right ordinate: c/deg) are plotted as a function of velocity (°/s) for Vernier discrimination (unfilled symbols) and letter resolution (filled symbols). Data plotted are the average values of the three observers. Error bars represent ± 1 S.D., including the variance both within and between the three observers.

discrimination and letter resolution, respectively. One possible way to interpret these results is that Vernier discrimination is mediated by *higher* spatial frequency mechanisms, which are more susceptible to the degradation produced by motion, blur and eccentricity, than letter resolution. However, our equivalent blur analysis is not consistent with this interpretation. As shown in Fig. 11, the estimated equivalent intrinsic blur is consistently lower for letter resolution at all velocities, implying that *lower* spatial-frequency mechanisms underlie Vernier discrimination. The difference between the estimated equivalent intrinsic blur for Vernier discrimination and letter resolution has another potential consequence. Because temporal frequency is a product of spatial frequency and velocity, the data in Fig. 11 imply that letter resolution can also tolerate higher temporal frequencies than Vernier discrimination. This implication was confirmed in a separate study [62].

What then, accounts for the basic differences between the two tasks? As noted above, it is widely held that *abutting* Vernier discrimination is mediated by the contrast responses of cortical spatial-filter mechanisms. Although these mechanisms are presumably involved also in processing letter targets, the results summarized in this and the previous section indicate that letter resolution may be limited by a different aspect of the responses of the filter-mechanisms or at a different stage of visual processing. Further experiments to identify the mechanisms that determine letter resolution are necessary in order to understand the differences that exist between Vernier discrimination and letter resolution.

Acknowledgements

We thank Chris Kuether for help in constructing the apparatus and Thanh Nguyen for assistance with 'psychoflexing'. We are grateful to Nancy Coletta, Dennis Levi and Haluk Ögmen for their helpful suggestions at various stages of this work. This study was supported in part by an Ezell Fellowship from the American Optometric Foundation, a Grant-in-Aid of Research from Sigma Xi, a Vision Research Support Grant and a Senior Graduate Student Fellowship from the University of Houston College of Optometry to STLC, Research Grant R01-EY05068 from the National Eye Institute to HEB and Core Center Grant P30-EY07551 from the National Eye Institute to the University of Houston College of Optometry.

References

[1] Westheimer G, McKee SP. Visual acuity in the presence of retinal image motion. J Opt Soc Am 1975;65:847–50.
[2] Ludvigh EJ. Visual acuity while one is viewing a moving object. Arch Ophthalmol 1949;42:14–22.
[3] Brown B. Resolution thresholds for moving targets at the fovea and in the peripheral retina. Vis Res 1972;12:293–304.
[4] Barnes GR, Smith R. The effects on visual discrimination of image movement across the stationary retina. Aviation, Space Environ Med 1981;52:466–72.
[5] Morgan MJ, Watt RJ, McKee SP. Exposure duration affects the sensitivity of vernier acuity to target motion. Vis Res 1983;23:541–6.
[6] Chung STL, Levi DM, Bedell HE. Vernier in motion: what accounts for the threshold elevation? Vis Res 1996;36:2395–410.
[7] Robson JG. Spatial and temporal contrast-sensitivity functions of the visual system. J Opt Soc Am 1966;56:1141–2.
[8] Kelly DH. Motion and vision. II. Stabilized spatio-temporal threshold surface. J Opt Soc Am 1979;69:1340–9.
[9] Kelly DH. Visual processing of moving stimuli. J Opt Soc Am A 1985;2:216–25.
[10] Koenderink JJ, van Doorn AJ. Spatiotemporal contrast detection threshold surface is bimodal. Optics Lett 1979;4:32–4.
[11] Burr DC, Ross J. Contrast sensitivity at high velocities. Vis Res 1982;22:479–84.
[12] Levi DM, Waugh SJ. Spatial scale shifts in peripheral Vernier acuity. Vis Res 1994;34:2215–38.
[13] Levi DM, Waugh SJ, Beard BL. Spatial scale shifts in amblyopia. Vis Res 1994;34:3315–33.
[14] Morgan MJ, Aiba TS. Vernier acuity predicted from changes in the light distribution of the retinal image. Spatial Vis 1985;1:151–61.
[15] Krauskopf J, Farell B. Vernier acuity: effects of chromatic content, blur and contrast. Vis Res 1991;31:735–49.
[16] Morgan MJ. Hyperacuity. In: Regan D, editor. Spatial Vision. London: Macmillan, 1991:87–113.
[17] Morgan MJ, Castet E. Stereoscopic depth perception at high velocities. Nature 1995;378:380–3.
[18] Levi DM. Pattern perception at high velocities. Curr Biol 1996;6:1020–4.
[19] Chung STL, Bedell HE. Moving Vernier with band-pass filtered stimuli. Invest Ophthalmol Vis Sci 1996;37:S734.
[20] Ludvigh EJ. Effect of reduced contrast on visual acuity as measured with Snellen test letters. Arch Ophthalmol 1941;25:469–74.
[21] Herse PR, Bedell HE. Contrast sensitivity for letter and grating targets under various stimulus conditions. Optom Vis Sci 1989;66:774–81.
[22] Waugh SJ, Levi DM. Visibility, timing and Vernier acuity. Vis Res 1993;33:505–26.
[23] Williams RA, Enoch JM, Essock EA. The resistance of selected hyperacuity configurations to retinal image degradation. Invest Ophthalmol Vis Sci 1984;25:389–99.
[24] Legge GE, Pelli DG, Rubin GS, Schleske MM. Psychophysics of reading. I. Normal vision. Vis Res 1985;25:239–52.
[25] Braje WL, Tjan BS, Legge GE. Human efficiency for recognizing and detecting low-pass filtered objects. Vis Res 1995;35:2955–66.
[26] Chung STL, Levi DM, Bedell HE. Ricco's diameter for line detection increases with stimulus velocity. J Opt Soc Am A 1996;13:2129–34.
[27] Klein SA. An Excel macro for transformed and weighted averaging. Behav Res Methods Instruments Computers 1992;24:90–6.
[28] Morgan MJ, Benton S. Motion-deblurring in human vision. Nature 1989;340:385–6.
[29] Barlow HB. Retinal noise and absolute threshold. J Opt Soc Am 1956;46:634–9.
[30] Barlow HB. Increment thresholds at low intensities considered as signal/noise discrimination. J Physiol 1957;136:469–88.
[31] Watt RJ, Morgan MJ. Spatial filters and the localization of luminance changes in human vision. Vis Res 1984;24:1387–97.
[32] Watt RJ, Hess RF. Spatial information and uncertainty in anisometropic amblyopia. Vis Res 1987;27:661–74.
[33] Levi DM, Klein SA. Equivalent intrinsic blur in spatial vision. Vis Res 1990;30:1971–93.
[34] Pelli DG. The quantum efficiency of vision. In: Blakemore C, editor. Vision: Coding and Efficiency. New York: Cambridge University Press, 1990:3–24.
[35] Waugh SJ, Levi DM, Carney T. Orientation, masking, and vernier acuity for line targets. Vis Res 1993;33:1619–38.
[36] Howland B, Ginsburg A, Campbell F. High-pass spatial frequency letters as clinical optotypes. Vis Res 1978;18:1063–6.
[37] Alexander KR, Xie W, Derlacki DJ. Spatial-frequency characteristics of letter identification. J Opt Soc Am A 1994;11:2375–82.
[38] Riggs LA. Visual acuity. In: Graham CH, editor. Vision and Visual Perception. New York: John Wiley and Sons, 1965:321–49.
[39] Westheimer G. Visual acuity. In: Hart WM Jr, editor. Adler's Physiology of the Eye. St. Louis: Mosby-Year Book, 1992:531–47.
[40] Bondarko VM, Danilova MV. What spatial frequency do we use to detect the orientation of a Landolt C? Vis Res 1997;37:2153–6.
[41] Weymouth FW. Effect of age on visual acuity. In: Hirsch MJ, Wick RE, editors. Vision of the Aging Patient. Philadelphia: Chilton, 1960:37–62.
[42] Wilson HR. Responses of spatial mechanisms can explain hyperacuity. Vis Res 1986;26:453–69.
[43] Levi DM, Klein SA, Aitsebaomo AP. Vernier acuity, crowding and cortical magnification. Vis Res 1985;25:963–77.
[44] Virus V, Näsänen R, Osmoviita K. Cortical magnification and peripheral vision. J Opt Soc Am A 1987;4:1568–78.
[45] Wilson HR. Model of peripheral and amblyopic hyperacuity. Vis Res 1991;31:967–82.
[46] Waugh SJ, Levi DM. Visibility, luminance and Vernier acuity. Vis Res 1993;33:527–38.
[47] Toet A, Levi DM. The two-dimensional shape of spatial interaction zones in the parafovea. Vis Res 1992;32:1349–57.
[48] Henderson CJ, Halmagyi GM, Curthoys IS. Visual acuity and gaze precision. In: Keller EL, Zee DS, editors. Adaptive Processes in Visual and Oculomotor Systems. New York: Pergamon Press, 1986:367–71.

[49] Chung STL, Bedell HE. Velocity criteria for 'foveation periods' determined from image motions simulating congenital nystagmus. Optom Vis Sci 1996;73:92–103.
[50] Demer, JL. Dynamic visual acuity during vertical retinal image motion: Comparison of normal and low vision. In: Vision Science and its Applications, vol 1, OSA Technical Digest Series. Washington, DC: OSA, 1995:214–17.
[51] Legge GE, Mullen KT, Woo GC, Campbell FW. Tolerance to visual defocus. J Opt Soc Am A 1987;4:851–63.
[52] Ludvigh EJ. Extrafoveal visual acuity as measured with Snellen test-letters. Am J Ophthalmol 1941;24:303–10.
[53] Campbell FW, Robson JG. Application of Fourier analysis to the visibility of gratings. J Physiol 1968;197:551–66.
[54] Blakemore C, Campbell FW. On the existence of neurons in the human visual system selectively sensitive to the orientation and size of retinal images. J Physiol 1969;203:237–60.
[55] Braddick O, Campbell FW, Atkinson J. Channels in vision: Basic aspects. In: Held R, Leibowitz HW, Teuber H-L, editors. Handbook of Sensory Physiology VIII: Perception. New York: Springer-Verlag, 1978:3–38.
[56] Legge GE, Foley JM. Contrast masking in human vision. J Opt Soc Am 1980;70:1458–71.
[57] DeValois RL, Albrecht DG, Thorell LG. Spatial frequency selectivity of cells in macaque visual cortex. Vis Res 1982;22:545–59.
[58] Wilson HR, McFarlane DK, Phillips GC. Spatial frequency tuning of orientation selective units estimated by oblique masking. Vis Res 1983;23:873–82.
[59] Kelly DH. Spatial frequency selectivity in the retina. Vis Res 1975;15:665–72.
[60] Legge GE, Rubin GS, Luebker A. Psychophysics of reading. V. The role of contrast in normal vision. Vis Res 1987;27:1165–77.
[61] Ho A, Bilton SM. Low contrast charts effectively differentiate between types of blur. Am J Optom Physiol Optics 1986;63:202–8.
[62] Chung, STL. Effect of image motion on spatial processing. Doctoral Dissertation, University of Houston, 1995.